

Are we done with ImageNet?

Lucas Beyer^{1*} Olivier J. Hénaff^{2*} Alexander Kolesnikov^{1*} Xiaohua Zhai^{1*} Aäron van den Oord^{2*}

¹Google Brain (Zürich, CH) and ²DeepMind (London, UK)

Abstract

Yes, and no. We ask whether recent progress on the ImageNet classification benchmark continues to represent meaningful generalization, or whether the community has started to overfit to the idiosyncrasies of its labeling procedure. We therefore develop a significantly more robust procedure for collecting human annotations of the ImageNet validation set. Using these new labels, we reassess the accuracy of recently proposed ImageNet classifiers, and find their gains to be substantially smaller than those reported on the original labels. Furthermore, we find the original ImageNet labels to no longer be the best predictors of this independently-collected set, indicating that their usefulness in evaluating vision models may be nearing an end. Nevertheless, we find our annotation procedure to have largely remedied the errors in the original labels, reinforcing ImageNet as a powerful benchmark for future research in visual recognition³.

1 Introduction

For nearly a decade, the ILSVRC image classification benchmark [1], “ImageNet”, has been a central testbed of research in artificial perception. In particular, its scale and difficulty have highlighted landmark achievements in machine learning, starting with the breakthrough AlexNet [2]. Importantly, success on ImageNet has often proven to be general: techniques that advance its state-of-the-art have usually been found to be successful in other tasks and domains. For example, progress on ImageNet due to architecture design [2, 3, 4] or optimization [5] has yielded corresponding gains on other tasks and modalities [6, 7, 8]. Similarly, successful representation learning techniques applied to ImageNet [9, 10, 11] have yielded corresponding gains elsewhere [12, 13, 14, 15].

As recent results continue to report systematic gains on ImageNet, we ask whether this progress continues to be as general as before. We therefore develop a method for collecting human annotations which leverages the predictions of a diverse set of image models, and use these Reassessed Labels (“ReaL”) to re-evaluate recent progress in image classification. While early progress on ImageNet almost perfectly

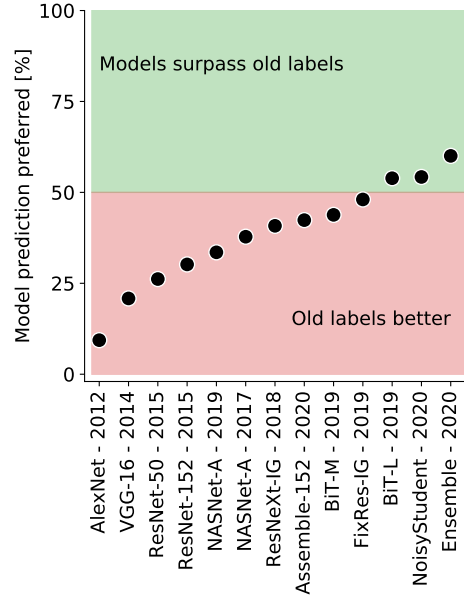


Figure 1: When presented with a model’s prediction and the original ImageNet label, human annotators now prefer model predictions on average (Section 4). Nevertheless, there remains considerable progress to be made before fully capturing human preferences.

* All authors contributed equally, project led by first author.

Correspondence: {lbeyer, henaff, akolesnikov, xzhai, avdnoord}@google.com

³The new labels and rater answers are available at <https://github.com/google-research/reassessed-imagenet>

translates into corresponding gains in ReAL accuracy, we find this association to be significantly weaker for more recent models. Surprisingly, we find the original ImageNet labels to no longer be the best predictors of our newly-collected annotations, with recent high-performing models systematically outperforming them (Figure 1). Next, we analyse the discrepancies between ImageNet and ReAL accuracy, finding that some of the “progress” on the original metric is due to overfitting to the idiosyncrasies of their labeling pipeline. Finally, we leverage these observations to propose two simple techniques which address the complexity of ImageNet scenes, leading to systematic gains in both ImageNet and ReAL accuracy.

Related work. Several studies have revisited common computer vision benchmarks [16, 17, 18, 19] and, regarding ImageNet [1] specifically, identified various sources of bias and noise [20, 21, 22]. However, none of these investigate the effect of ImageNet’s shortcomings, in particular how they might affect model accuracies and conclusions being drawn from them. The most related recent work [23] attempts to replicate the ImageNet collection pipeline, which results in a 12% drop in accuracy. However, they eventually conclude that accuracy gains on the original validation set perfectly translate to their newly collected data. Later, [24] demonstrate that this discrepancy is explained by a statistical bias in the data collection process that was unintentionally introduced in the replication. Regardless, we significantly differ from this line of work, as we do not collect new images, but rather identify shortcomings of the existing validation labels and collect a new label set which addresses these. ObjectNet [25] is another work that collects a new validation set that can be used to evaluate ImageNet models, focusing on gathering challenging “real-life” images in diverse contexts. It also significantly differs from our work, as ObjectNet images introduces a strong domain shift, which is orthogonal to our enquiry. Concurrently with our work, [26] proposes an improved pipeline for collecting ImageNet labels, although their analysis and conclusions differ from ours.

2 What is wrong with ImageNet labels?

The ImageNet dataset is a landmark achievement in the evaluation of machine learning techniques. In particular, the ImageNet labeling pipeline allows for human judgments in a 1000-way real-world image classification task, an intractable problem using a naive interface. Nevertheless, this procedure has some limitations which we seek to identify. Many images in the ImageNet dataset contain a clear view on a single object of interest: for these, a single label is an appropriate description of their content. However many other images contain multiple, similarly prominent objects, limiting the relevance of a single label. Even for images containing a single object, biases in the collection procedure can lead to systematic inaccuracies. Finally, some ImageNet classes are inherently ambiguous, drawing distinctions between essentially identical groups of images. In this section we review these sources of label noise, which motivate the design of a new human annotation procedure.

Single label per image. Real-world images often contain multiple objects of interest. Yet, ImageNet annotations are limited to assigning a single label to each image, which can lead to a gross under-representation of the content of an image (Figure 2, top row). In these cases, the ImageNet label is just one of many equally valid descriptions of the image, chosen in a way that reflects the idiosyncrasies of the labeling pipeline more than the content of the image. As a result, using ImageNet validation accuracy as a metric can penalize an image classifier for producing a correct description that happens to not coincide with that chosen by the ImageNet label. This motivates re-annotating the ImageNet validation set in a way that captures the diversity of image content in real-world scenes.

Overly restrictive label proposals. The ImageNet annotation pipeline consists of querying the internet for images of a given class, then asking human annotators whether that class is indeed present in the image. While this procedure yields reasonable descriptions of the image, it can also lead to inaccuracies. When considered in isolation, a particular label proposal can appear to be a plausible description of an image (Figure 2, middle row). Yet when considered together with other ImageNet classes, this description immediately appears less suitable (the “quill” is in fact a “feather boa”, the “passenger car” a “school bus”). Based on this observation, we seek to design a labeling procedure which allows human annotators to consider (and contrast) a wide variety of potential labels, so as to select the most accurate description(s).

Arbitrary class distinctions. ImageNet classes contain a handful of *essentially* duplicate pairs, which draw a distinction between semantically and visually indistinguishable groups of images (Figure 2, bottom row). For example, the original ImageNet labels distinguish “sunglasses” from

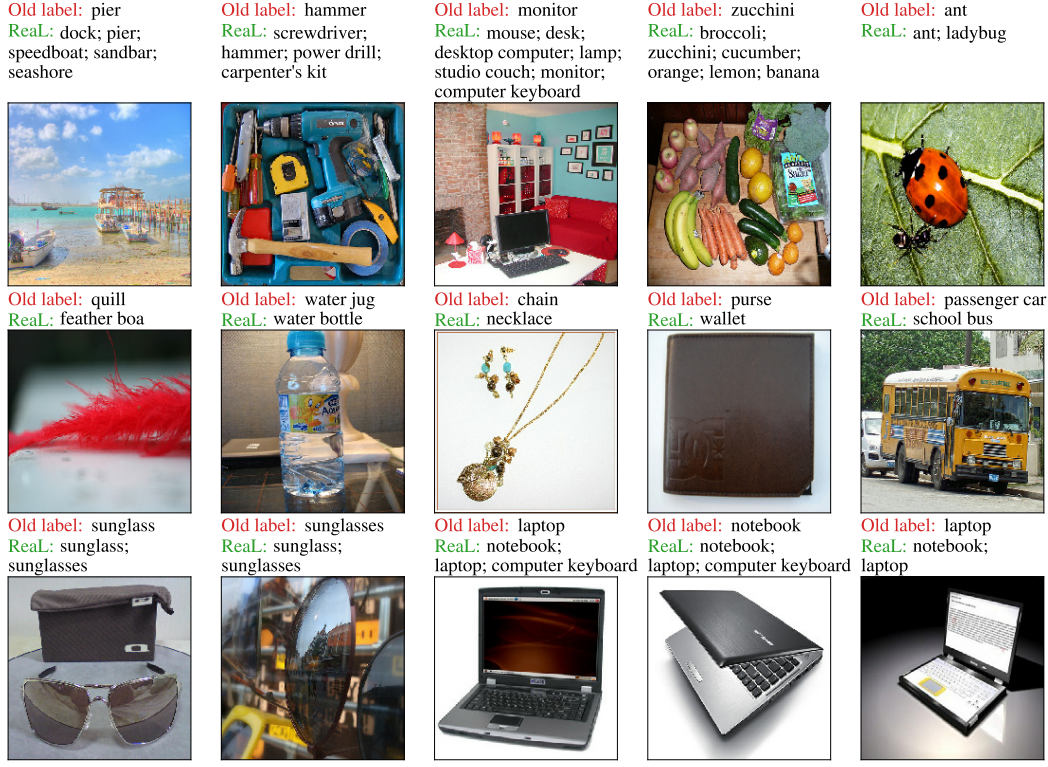


Figure 2: Example failures of the ImageNet labeling procedure. Red: original ImageNet label, green: proposed ReaL labels. **Top row:** ImageNet currently assigns a single label per image, yet these often contain several equally prominent objects. **Middle row:** Even when a single object is present, ImageNet labels present systematic inaccuracies due to their labeling procedure. **Bottom row:** ImageNet classes contain a few unresolvable distinctions.

“sunglass”, “laptop” from “notebook”, and “projectile, missile” from “missile”. By allowing multiple annotations from simultaneously-presented label proposals, we seek to remove this ambiguity and arrive at a more meaningful metric of classification performance.

3 Relabeling the ImageNet validation set

Given the biases arising from assigning a single label in isolation, we design a labeling procedure which captures the diversity and multiplicity of content in the ImageNet dataset. In particular, we seek a paradigm which allows human annotators to simultaneously evaluate a diverse set of candidate labels, while keeping the number of proposals sufficiently small to enable robust annotations.

3.1 Collecting a comprehensive set of proposals

We start by assembling a set of 19 models [3, 27, 4, 28, 29, 30, 31, 32, 33, 34, 35, 36, 37] which vary along a number of dimensions, including architecture, training objective and usage of external data (see appendix A). We use either a canonical public implementation, or predictions provided by the authors. In order to generate label proposals from these models we adopt the following strategy: for any given image, we always include the original ImageNet (ILSVRC-2012) label and the Top-1 prediction of each model. Moreover, given that many images may have more than one label, we allow each model to make additional proposals based on the logits and probabilities it assigns across the entire dataset (see appendix A). We find this procedure for generating label proposals to result in near perfect label coverage, at the expense of having a very large number of proposed labels per image.

In order to reduce the number of proposals, we seek a small subset of models whose proposals retain a near perfect label coverage. In order to quantify the precision and recall of a given subset, we had 256 images labeled by 5 computer vision experts, which we use as *gold standard*. We then perform

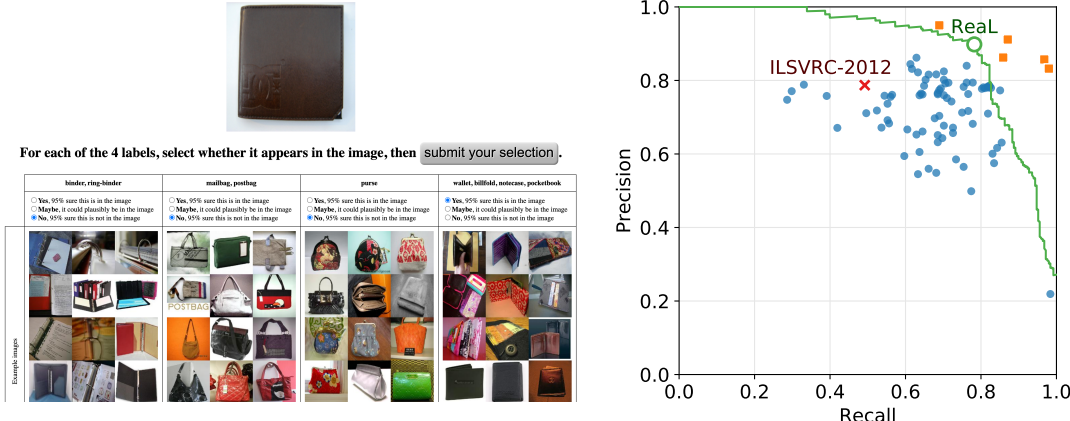


Figure 3: Human assessment of proposed labels. **Left:** the interface for simultaneous evaluation of multiple label proposals. **Right:** precision and recall of individual raters (blue dots), expert annotators (orange boxes), and the model fit to rater data (green curve), evaluated on a majority-vote from expert annotators. The labels we use for subsequent analyses are indicated by a green circle, the original ImageNet labels with a red cross.

an exhaustive search over model subsets to find a group which achieves the highest precision, while maintaining a recall above 97%. Based on this, we find a subset of 6 models which generates label proposals that have a recall of 97.1% and a precision of 28.3%, lowering the average number of proposed labels from 13 per image to 7.4 per image. From this subset, we generate proposal labels for the entire validation set, using the same rule as described above.

3.2 Human evaluation of proposed labels

Having obtained a new set of candidate labels for the entire validation set, we start by assessing which images need to be evaluated by human raters. In the event that all models agree with the original ImageNet label, we can safely retain the original without re-evaluation. This reduces the number of images to be annotated from 50 000 to 24 889. To avoid overwhelming raters with choices, we further split images with more than 8 label proposals into multiple labeling tasks according to the WordNet hierarchy. This results in 37 988 labeling tasks.

Each task is performed by 5 separate human annotators, using a crowdsourcing platform. On a given trial a rater is presented with a single image and up to 8 candidate labels, and asked whether each label is present in the image (Figure 3, left). For each label, the rater is instructed to respond yes if they are 95% sure that the label is indeed present in the image, no if they are 95% sure that the label is not present in the image, and maybe otherwise.

3.3 From human ratings to labels and a metric

The next step is to combine the 5 human assessments of every proposed label into a single binary decision of whether to retain or discard it. In order to account for raters’ varying characteristics, we use the classic method by Dawid and Skene [38] which infers individual rater’s error rates via maximum-likelihood. We note that animal classes often carry more uncertainty and require expert opinion, which the original ImageNet labels indirectly incorporate via expert websites. We therefore incorporate the ImageNet label as a virtual 6th rater for images originally labeled as animals. The precision-recall curve resulting from the whole process is shown in Figure 3 (right). We also tried simple majority voting, which performs well but worse: 90.8% precision and 71.8% recall. The operating point we choose, marked by a circle on the curve, results in 57 553 labels for 46 837 images. We discard the 3163 images that are assigned no label.

Equipped with these new validation set labels we propose a new metric: the RealL accuracy (from Reassessed Labels), which addresses some of the shortcomings of the original ImageNet accuracy identified in Section 2. In particular, we wish to no longer penalise models for predicting one of multiple plausible labels of an image. We therefore measure the precision of the model’s top-1 prediction, which is deemed correct if it is included in the set of labels, and incorrect otherwise.

4 Re-evaluating the state of the art

Using the proposed ReAL accuracy, we now re-assess the progress of recently proposed classifiers on the ImageNet dataset. In particular, given the strong generalization shown by early models (Section 1) we would expect ImageNet accuracy to be very predictive of ReAL accuracy for these models. This was indeed the case: when regressing ImageNet accuracy onto ReAL accuracy for the first half (ordered by ImageNet accuracy) of our models, we found a strong linear relationship (Figure 4, solid line: slope = 0.86). When fitting the accuracies of more recent models (the second half), we again found a strong linear relationship, however its slope was significantly reduced (Figure 4, dashed line: slope = 0.51; $p < 0.001$, Z-test on the difference in slopes). Importantly, several models [30, 39] already surpass the ReAL accuracy obtained by the original ImageNet labels (Figure 4, red point and dashed line). Together with the weakening relationship between ImageNet and ReAL accuracy, this suggests that we may be approaching the end of their utility as an evaluation metric.

In order to confirm this trend, we directly ask whether ReAL labels are better predicted by model outputs or ImageNet labels. We search for all images in which the ImageNet label disagrees with a given model’s prediction (i.e. “mistakes” according to the original ImageNet metric), and ask which is deemed correct by the ReAL labels. If the ReAL label considers both (model and ImageNet) predictions correct or incorrect, we discard the image. We then compute the proportion of remaining images whose model-predicted label is considered correct. The results of this analysis are very consistent with our previous finding: while early models are considerably worse than ImageNet labels at predicting human preferences, recent models now surpass them (Figure 1).

To see if these trends continue even further with higher ImageNet accuracy, we also created an ensemble of the three best models by combining their logits. The resulting model reaches 89.0% in original ImageNet accuracy, and 91.20% ReAL accuracy, furthering outperforming ImageNet labels according to human preferences (Figure 1).

4.1 Beyond single label predictions

The ReAL accuracy metric assesses whether a model’s single most confident prediction falls within the set of acceptable answers. However, a more stringent criterion would ask whether all of the model’s top predictions fall within this acceptable set. Given that our models are trained with a single label per image, these secondary predictions could very well be unconstrained and fairly meaningless. On the other hand, the visual similarity between classes could mean that an increase in accuracy of the top prediction will also entail an increase for later predictions.

Figure 5 shows that the accuracy of models’ second and third predictions are significantly lower than their first. Nevertheless, these predictions remain far superior to what would be expected due to chance, indicating that the correlations across classes enable meaningful secondary predictions. Furthermore, these secondary accuracies display a striking correlation with the primary accuracy, indicating that it may be sufficient to improve upon the top-1 ReAL

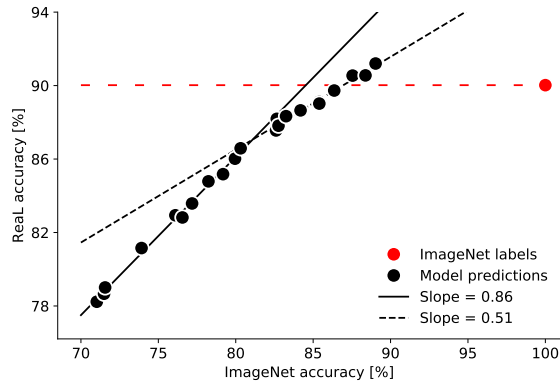


Figure 4: Comparing progress on ReAL accuracy and the original ImageNet accuracy. We measured the association between both metrics by regressing ImageNet accuracy onto ReAL accuracy for the first (solid line) and second half (dashed line) of the models in our pool.

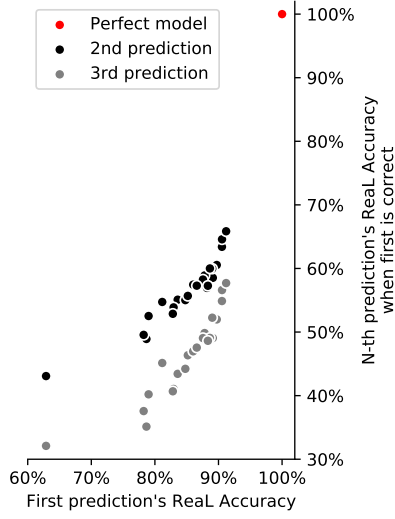


Figure 5: ReAL accuracy of models’ 2nd and 3rd predictions.

Table 1: ImageNet classes that often co-occur with other classes. The table presents class-level accuracies for different models. Current top-performing models outperform "Ideal" model that picks a correct label for each image at random. The last column shows top co-occurring classes, the number in brackets indicates percentage of how often a certain label co-occurs.

ImageNet class	"Oracle" model	Noisy Student	Assemble R152	VGG16	Top co-occurring classes
desktop comp.	29.9%	71.1%	71.1%	60.0%	monitor (87%) ; keyboard (78%)
muzzle	73.8%	100.0%	90.0%	55.0%	german shepherd (5%) ; holster (5%)
convertible	73.0%	97.6%	95.2%	78.6%	car wheel (40%) ; grille (17%)
cucumber	74.2%	93.2%	88.6%	70.5%	zucchini (20%) ; bell pepper (9%)
swing	87.5%	100.0%	94.0%	72.0%	chain (12%) ; sweatshirt (2%)

accuracy metric in order to also make progress on this more stringent task. We therefore consider ReAL accuracy to be a good default metric to be used for our new set of labels. Nevertheless, in the event that models start achieving near-perfect accuracy on this metric, it can easily be made more stringent by also accounting for secondary predictions.

4.2 An analysis of co-occurring classes

Among ImageNet images that we re-annotate with ReAL labels, approximately 29% either contain multiple objects or a category that corresponds to multiple synonym labels in ImageNet (Figure 2). This raises a natural question of how ImageNet models perform on such images. Do they predict one of the correct labels at random, or do they learn to exploit biases in the labeling procedure to guess the ImageNet label? In this section, we use our ReAL labels to study this question in depth.

We start by considering all images whose ImageNet label is included in the ReAL labels. Based on the ReAL labels, we compute the expected per-class accuracy of an “unbiased oracle” model, which predicts one of the ReAL labels uniformly at random. If there is no bias in the original ImageNet labeling procedure, the per-class accuracies of this model represent the highest achievable accuracy.

To focus on ambiguous classes which frequently co-occur with one another, we only consider classes for which the unbiased oracle achieves less than 90% accuracy. Some of these “ambiguous” classes could in fact be due to labeling noise, hence we also exclude fine-grained animal classes, as human raters frequently make mistakes on these. We are left with 253 classes that fit these criteria. These include ambiguous pairs such as (sunglass, sunglasses), (bathtub, tub), (promontory, cliff) and (laptop, notebook) (see Figure 2, bottom row), as well as classes which frequently appear together, e.g. (keyboard, desk), (cucumber, zucchini) and (hammer, nail), see (Figure 2, top row).

In Table 1 we illustrate this in more detail. For instance, the “desktop computer” category frequently co-occurs with many other categories: more than 75% of images that have a “desktop computer” also have a “monitor”, a “computer keyboard” and a “desk”. If there was no label bias, the highest achievable accuracy on the “desktop computer” category would be approximately 30%. However, we observe that both the Noisy Student and the Assemble-ResNet152 models achieve a significantly higher accuracy of 71.1%.

In Figure 6 we compare the distribution of class-level accuracies of all models from our study to the unbiased oracle. The figure demonstrates that recent top-performing models, such

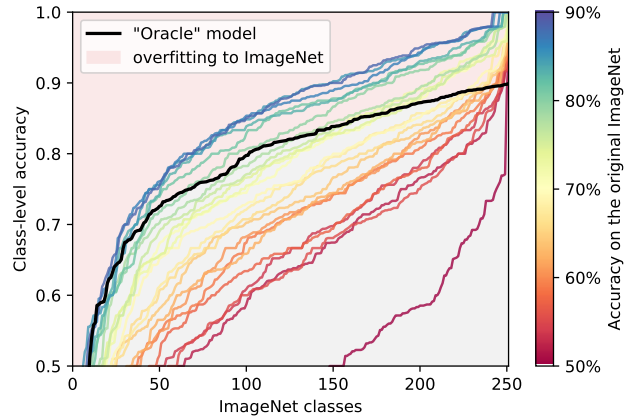


Figure 6: Each color curve corresponds to an ImageNet model and depicts sorted class-level accuracies. The black curve depicts accuracies of the “unbiased oracle”. Recent top-performing models dominate the oracle curve and, thus, are overfitting to label biases present in ImageNet.

as BiT-L and Noisy Student dominate the unbiased oracle model. This implies that a significant fraction of progress on ImageNet has been achieved by exploiting biases present in the ImageNet labeling procedure, and may explain why these gains only partially transfer to ReaL accuracy.

5 Analyzing the remaining mistakes

Even the highest-performing models display an error rate of approximately 11% according to ImageNet labels, and 9% according to ReaL labels. What is the nature of these mistakes, and what does this imply regarding the progress to be made on each of these benchmarks?

To answer these questions, we design a follow-up study which shows images and model predictions that are “mistakes” according to a particular metric (i.e. ImageNet labels or ReaL labels). To put these “mistakes” into context, we also show raters what the “correct” labels are for this image, as well as example images from those classes. We then instruct raters to identify the reason for the prediction being considered a mistake: is it indeed a mistake? Or is the prediction actually correct, and it is the label which is incorrect or incomplete? Or is it neither of these options, for example if the labels are of fine-grained classes which the rater cannot distinguish?⁴

We sort the models used in this study according to their ImageNet accuracy. Using this ordering, we can appreciate a systematic decrease in the number of “clear mistakes”, indicating that there is indeed genuine progress on both benchmarks (Figure 7, top row). Nevertheless, there remains a significant fraction of “mistakes” which are deemed correct by human raters (Figure 7, middle row). Importantly, these cases are much more frequent when sampling from ImageNet mistakes than ReaL mistakes, indicating that the ReaL labels have indeed remedied a large portion of these false negatives.

Finally, a non-negligible number of mistakes are considered to be “undecidable” by raters (Figure 7, bottom row). Indeed, certain fine-grained classes are often hard or impossible to differentiate by non-experts. For these, ImageNet labels and ReaL labels yield similar assessments of high-performing models, indicating that collecting annotations from human experts may be necessary to measure progress along this axis. In summary, while ReaL labels seem to be of comparable quality to ImageNet ones for fine-grained classes, they have significantly reduced the noise in the rest, enabling further meaningful progress on this benchmark.

6 Improving ImageNet training

We have identified two shortcomings of the ImageNet labeling procedure, both of which stem from assigning a single label to images which require multiple. As ImageNet training images were annotated using the same process, we would expect similar types of noise in their labels as well. In this section we investigate two ways of addressing this problem.

First, we propose using a training objective which allows models to emit multiple non-exclusive predictions for a given image. For this we investigate treating the multi-way classification problem as a set of independent binary classification problems, and penalizing each one with a sigmoid cross-entropy loss, which does not enforce mutually exclusive predictions.

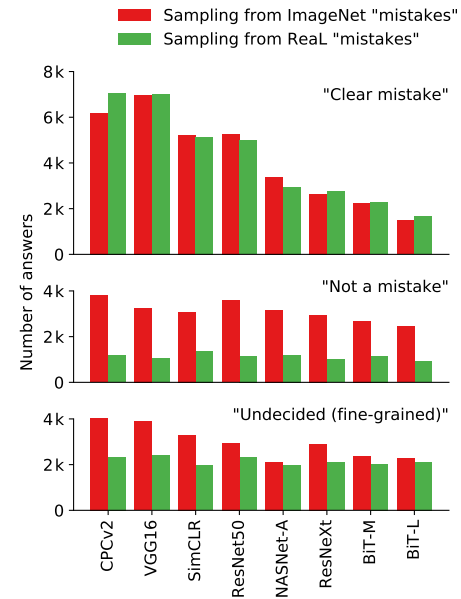


Figure 7: Remaining mistake types. We presented human raters with model predictions deemed incorrect according to either the ImageNet labels, or the ReaL labels, and asked them whether these predictions were indeed “clear mistakes”, in fact “not a mistake”, or simply “undecidable”.

⁴We had more options such as “illegible image” or “depiction of A as B”, but found that they were not used.

Table 2: Top-1 accuracy (in percentage) on ImageNet with our proposed sigmoid loss and clean label set. Median accuracy from three runs is reported for all the methods. Either sigmoid loss or clean label set leads to consistent improvements over baseline. Using both achieves the best performance. The improvement of our proposed method is more pronounced with longer training schedules.

Model	ImageNet accuracy			ReaL accuracy			
	90 epochs	270 epochs	900 epochs	90 epochs	270 epochs	900 epochs	
ResNet-50	Baseline	76.0	76.9 (+0.9)	75.9 (-0.1)	82.5	82.9 (+0.4)	81.6 (-0.9)
	+ Sigmoid	76.3 (+0.3)	77.8 (+1.8)	76.9 (+0.9)	83.0 (+0.5)	83.9 (+1.4)	82.7 (+0.2)
	+ Clean	76.4 (+0.4)	77.8 (+1.8)	77.4 (+1.4)	82.8 (+0.3)	83.7 (+1.2)	83.3 (+0.8)
	+ Both	76.6 (+0.6)	78.2 (+2.2)	78.5 (+2.5)	83.1 (+0.6)	84.3 (+1.8)	84.1 (+1.6)
ResNet-152	Baseline	78.0	78.3 (+0.3)	77.1 (-0.9)	84.1	83.8 (-0.3)	82.3 (-1.8)
	+ Sigmoid	78.5 (+0.5)	78.7 (+0.7)	77.4 (-0.6)	84.6 (+0.5)	84.3 (+0.2)	82.7 (-1.4)
	+ Clean	78.6 (+0.6)	79.6 (+1.6)	79.0 (+1.0)	84.4 (+0.3)	85.0 (+0.9)	84.4 (+0.3)
	+ Both	78.7 (+0.7)	79.8 (+1.8)	79.3 (+1.3)	84.6 (+0.5)	85.2 (+1.1)	84.5 (+0.4)

Second, based on our observation that recent top-performing models surpass the original ImageNet labels in their ability to predict human preferences (Figure 1), we asked whether we could use these models to filter the noise in ImageNet labels. We use one of the best models from our study, BiT-L, to clean the ImageNet training set. In order to counter memorization of training data, we split training images into 10 equally-sized folds. For each fold we perform the following: (1) Hold the fold out and train the BiT-L model on the remaining 9 folds and (2) Use the resulting model to predict labels on the hold-out fold. We then remove all images whose labels are inconsistent with BiT-L’s predictions. Through this procedure, we retain approximately 90% of the original training set.

Finally, we investigate these two techniques in the context of longer training schedules. This is inspired by [40], which observes that long training schedules can be harmful in the presence of noisy data. We therefore expect cleaning the ImageNet training set (or using the sigmoid loss) to yield additional benefits in this regime.

In Table 2, we present comprehensive empirical evaluation of ResNet models trained on ImageNet, which includes investigation into loss type (softmax vs. sigmoid), longer training and cleaned training data. Inspecting the table we draw multiple insights: (1) Training on clean ImageNet data consistently improves accuracy of the resulting model. The gains are more pronounced when the standard softmax loss is used. (2) Changing the softmax loss to the sigmoid loss also results in consistent accuracy improvements across all ResNet architectures and training settings. (3) Combining clean data and sigmoid loss leads to further improvements. (4) Finally, as opposed to the standard setting (softmax loss, full ImageNet data) which overfits for long schedules, training for longer using clean labels and sigmoid loss results in large gains.

A ResNet-50 architecture trained for 900 epochs with our proposed sigmoid loss on the clean training set achieves 78.5% top-1 accuracy, which improves by 2.5% over the standard ResNet-50 baseline (76.0%) as well as the 900-epoch baseline. Importantly, the gain in ReaL accuracy is 1.6%, despite the 900-epoch baseline heavily overfitting in terms of ReaL accuracy (-0.9%). We provide an extended table of results and plots in the Appendix B.

7 Conclusion

In this work, we investigated whether recent progress on the ImageNet benchmark amounts to meaningful generalization, or whether we have begun to overfit to artifacts in the validation set. To that end we identified a set of deficiencies in the original validation labels, and collected a new set of annotations which address these. Using these “Reassessed Labels” (ReaL), we found the association between progress on ImageNet and ReaL progress to have weakened over time, although it remains significant. Importantly, recent models have begun to surpass the original ImageNet labels in terms of their ReaL accuracy, indicating that we may be approaching the end of their usefulness. In a follow-up experiment, we found ReaL labels to remove more than half of the ImageNet labeling mistakes, implying that ReaL labels provide a superior estimate of the model accuracy.

Given the shortcomings of ImageNet labels we identified, we proposed two modifications to the canonical supervised training setup aimed at addressing them. Together, these simple modifications yield relatively large empirical gains, and indicate that label noise could have been a limiting factor for longer training schedules. Together, these findings suggest that although the original set of labels may be nearing the end of their useful life, ImageNet and its ReaL labels can readily benchmark progress in visual recognition for the foreseeable future.

Acknowledgements. We would like to thank every one of the raters involved in this task for their hard work, as well as their manager for making this a smooth experience. We also thank Pierre Ruyssen for engineering support in the initial phase of the project, and Ilya Tolstikhin for references and inspiration regarding the longer training schedules in Section 6. Finally, we are thankful to Tobias Weyand for his thorough review of a draft of this paper.

References

- [1] Olga Russakovsky, Jia Deng, Hao Su, Jonathan Krause, Sanjeev Satheesh, Sean Ma, Zhiheng Huang, Andrej Karpathy, Aditya Khosla, Michael Bernstein, et al. Imagenet large scale visual recognition challenge. *IJCV*, 2015.
- [2] Alex Krizhevsky, Ilya Sutskever, and Geoffrey E Hinton. Imagenet classification with deep convolutional neural networks. In *NeurIPS*, 2012.
- [3] Karen Simonyan and Andrew Zisserman. Very deep convolutional networks for large-scale image recognition. *arXiv preprint arXiv:1409.1556*, 2014.
- [4] Kaiming He, Xiangyu Zhang, Shaoqing Ren, and Jian Sun. Deep residual learning for image recognition. In *CVPR*, 2016.
- [5] Sergey Ioffe and Christian Szegedy. Batch normalization: Accelerating deep network training by reducing internal covariate shift. *arXiv preprint arXiv:1502.03167*, 2015.
- [6] Ashish Vaswani, Noam Shazeer, Niki Parmar, Jakob Uszkoreit, Llion Jones, Aidan N Gomez, Łukasz Kaiser, and Illia Polosukhin. Attention is all you need. In *NeurIPS*, 2017.
- [7] Aaron van den Oord, Sander Dieleman, Heiga Zen, Karen Simonyan, Oriol Vinyals, Alex Graves, Nal Kalchbrenner, Andrew Senior, and Koray Kavukcuoglu. Wavenet: A generative model for raw audio. *arXiv preprint arXiv:1609.03499*, 2016.
- [8] David Silver, Julian Schrittwieser, Karen Simonyan, Ioannis Antonoglou, Aja Huang, Arthur Guez, Thomas Hubert, Lucas Baker, Matthew Lai, Adrian Bolton, et al. Mastering the game of go without human knowledge. *Nature*, 550(7676), 2017.
- [9] Aaron van den Oord, Yazhe Li, and Oriol Vinyals. Representation learning with contrastive predictive coding. *arXiv preprint arXiv:1807.03748*, 2018.
- [10] Mathilde Caron, Piotr Bojanowski, Armand Joulin, and Matthijs Douze. Deep clustering for unsupervised learning of visual features. In *ECCV*, 2018.
- [11] Chengxu Zhuang, Alex Lin Zhai, and Daniel Yamins. Local aggregation for unsupervised learning of visual embeddings. In *ICCV*, 2019.
- [12] Tengda Han, Weidi Xie, and Andrew Zisserman. Video representation learning by dense predictive coding. In *ICCV Workshops*, 2019.
- [13] Steffen Schneider, Alexei Baevski, Ronan Collobert, and Michael Auli. wav2vec: Unsupervised pre-training for speech recognition. *arXiv preprint arXiv:1904.05862*, 2019.
- [14] Humam Alwassel, Dhruv Mahajan, Lorenzo Torresani, Bernard Ghanem, and Du Tran. Self-supervised learning by cross-modal audio-video clustering. *arXiv preprint arXiv:1911.12667*, 2019.
- [15] Chengxu Zhuang, Tianwei She, Alex Andonian, Max Sobol Mark, and Daniel Yamins. Unsupervised learning from video with deep neural embeddings. *arXiv preprint arXiv:1905.11954*, 2019.

- [16] Filip Radenović, Ahmet Iscen, Giorgos Tolias, Yannis Avrithis, and Ondřej Chum. Revisiting oxford and paris: Large-scale image retrieval benchmarking. In *CVPR*, 2018.
- [17] Björn Barz and Joachim Denzler. Do we train on test data? purging cifar of near-duplicates. *arXiv preprint arXiv:1902.00423*, 2019.
- [18] Tobias Weyand, Andre Araujo, Bingyi Cao, and Jack Sim. Google landmarks dataset v2—a large-scale benchmark for instance-level recognition and retrieval. *arXiv preprint arXiv:2004.01804*, 2020.
- [19] Kevin Musgrave, Serge Belongie, and Ser-Nam Lim. A metric learning reality check. *arXiv preprint arXiv:2003.08505*, 2020.
- [20] Curtis G Northcutt, Lu Jiang, and Isaac L Chuang. Confident learning: Estimating uncertainty in dataset labels. *arXiv preprint arXiv:1911.00068*, 2019.
- [21] Sara Hooker, Aaron Courville, Yann Dauphin, and Andrea Frome. Selective brain damage: Measuring the disparate impact of model pruning. *arXiv preprint arXiv:1911.05248*, 2019.
- [22] Pierre Stock and Moustapha Cisse. Convnets and imagenet beyond accuracy: Understanding mistakes and uncovering biases. In *ECCV*, 2018.
- [23] Benjamin Recht, Rebecca Roelofs, Ludwig Schmidt, and Vaishaal Shankar. Do imagenet classifiers generalize to imagenet? *arXiv preprint arXiv:1902.10811*, 2019.
- [24] Logan Engstrom, Andrew Ilyas, Shibani Santurkar, Dimitris Tsipras, Jacob Steinhardt, and Aleksander Madry. Identifying statistical bias in dataset replication. *arXiv preprint arXiv:2005.09619*, 2020.
- [25] Andrei Barbu, David Mayo, Julian Alverio, William Luo, Christopher Wang, Dan Gutfreund, Josh Tenenbaum, and Boris Katz. Objectnet: A large-scale bias-controlled dataset for pushing the limits of object recognition models. In *NeurIPS*, 2019.
- [26] Dimitris Tsipras, Shibani Santurkar, Logan Engstrom, Andrew Ilyas, and Aleksander Madry. From imagenet to image classification: Contextualizing progress on benchmarks. *arXiv preprint arXiv:2005.11295*, 2020.
- [27] Christian Szegedy, Vincent Vanhoucke, Sergey Ioffe, Jon Shlens, and Zbigniew Wojna. Rethinking the inception architecture for computer vision. In *CVPR*, 2016.
- [28] Saining Xie, Ross Girshick, Piotr Dollár, Zhuowen Tu, and Kaiming He. Aggregated residual transformations for deep neural networks. In *CVPR*, 2017.
- [29] Dhruv Mahajan, Ross Girshick, Vignesh Ramanathan, Kaiming He, Manohar Paluri, Yixuan Li, Ashwin Bharambe, and Laurens van der Maaten. Exploring the limits of weakly supervised pretraining. In *ECCV*, 2018.
- [30] Alexander Kolesnikov, Lucas Beyer, Xiaohua Zhai, Joan Puigcerver, Jessica Yung, Sylvain Gelly, and Neil Houlsby. Big transfer (BiT): General visual representation learning. *arXiv preprint arXiv:1912.11370*, 2019.
- [31] Jungkyu Lee, Taeryun Won, and Kiho Hong. Compounding the performance improvements of assembled techniques in a convolutional neural network. *arXiv preprint arXiv:2001.06268*, 2020.
- [32] Barret Zoph, Vijay Vasudevan, Jonathon Shlens, and Quoc V Le. Learning transferable architectures for scalable image recognition. In *CVPR*, 2018.
- [33] Han Cai, Chuang Gan, and Song Han. Once for all: Train one network and specialize it for efficient deployment. *arXiv preprint arXiv:1908.09791*, 2019.
- [34] Xiaohua Zhai, Avital Oliver, Alexander Kolesnikov, and Lucas Beyer. S4L: Self-supervised semi-supervised learning. In *ICCV*, 2019.

- [35] Olivier J Hénaff, Aravind Srinivas, Jeffrey De Fauw, Ali Razavi, Carl Doersch, SM Eslami, and Aaron van den Oord. Data-efficient image recognition with contrastive predictive coding. *arXiv preprint arXiv:1905.09272*, 2019.
- [36] Xinlei Chen, Haoqi Fan, Ross Girshick, and Kaiming He. Improved baselines with momentum contrastive learning. *arXiv preprint arXiv:2003.04297*, 2020.
- [37] Ting Chen, Simon Kornblith, Mohammad Norouzi, and Geoffrey Hinton. A simple framework for contrastive learning of visual representations. *arXiv preprint arXiv:2002.05709*, 2020.
- [38] Alexander Philip Dawid and Allan M Skene. Maximum likelihood estimation of observer error-rates using the em algorithm. *Journal of the Royal Statistical Society: Series C (Applied Statistics)*, 28(1):20–28, 1979.
- [39] Qizhe Xie, Eduard Hovy, Minh-Thang Luong, and Quoc V Le. Self-training with noisy student improves imagenet classification. *arXiv preprint arXiv:1911.04252*, 2019.
- [40] Devansh Arpit, Stanisław Jastrzębski, Nicolas Ballas, David Krueger, Emmanuel Bengio, Maxinder S Kanwal, Tegan Maharaj, Asja Fischer, Aaron Courville, Yoshua Bengio, and Simon Lacoste-Julien. A closer look at memorization in deep networks. In *JMLR*, 2017.
- [41] Hugo Touvron, Andrea Vedaldi, Matthijs Douze, and Hervé Jégou. Fixing the train-test resolution discrepancy. In *NeurIPS*, 2019.

A Details on proposal generation

The exact algorithm for the label proposal rule is as follows: for each model, compute its logits and probabilities for each image, resulting in two times 50 M image-label pairs. From these, keep those that fall into the largest 150 k logits or the largest 150 k probabilities. Pool all of these from all models. Remove image-label pairs that have only been brought up a single time by a single model. For each image, unconditionally add each model’s top-1 prediction for each image, as well as the original ILSVRC-2012 label.

As mentioned in the main text, we first generate an exhaustive list of image-label proposals using all models shown in Table 3, have 5 computer vision experts label a subset of images using these proposals, and then select a subset of models (indicated in Table 3, “Final” column) that reaches an almost-perfect recall (97.08%) and significantly increases precision (from 14.55% to 28.33%) in order to reduce the labeling burden.

Table 3: The models used for label proposal in this study, and their characteristics.

Ref.	Model	Arch. search	Self-sup.	Ext. data	Final
[3]	VGG-16	no	no	no	yes
[27]	Inception v3	no	no	no	yes
[4]	ResNet-50	no	no	no	no
[4]	ResNet-152	no	no	no	no
[28]	ResNeXt-101, 32x8d	no	no	no	no
[29]	ResNeXt-101, 32x8d, IG	no	no	yes	yes
[29]	ResNeXt-101, 32x48d, IG	no	no	yes	no
[30]	BiT-M	no	no	yes	yes
[30]	BiT-L	no	no	yes	yes
[31]	Assemble ResNet-50	yes	no	no	no
[31]	Assemble ResNet-152	yes	no	no	no
[32]	NASNet-A Large	yes	no	no	no
[32]	NASNet-A Mobile	yes	no	no	no
[33]	Once for all (Large)	yes	no	no	no
[34]	S4L MOAM	no	yes	no	no
[35]	CPC v2, fine-tuned	no	yes	no	yes
[35]	CPC v2, linear	no	yes	no	no
[36]	MoCo v2, long	no	yes	no	no
[37]	SimCLR	no	yes	no	no

B Improving ImageNet training

Table 4: Top-1 accuracy (in percentage) on ImageNet with our proposed sigmoid loss and clean label set. Median accuracy from three runs is reported for all the methods. Either sigmoid loss or clean label set leads to consistent improvements over baseline. Using both achieves the best performance. The improvement of our proposed method is more pronounced with longer training schedules.

Model	ImageNet accuracy			ReaL accuracy			
	90 epochs	270 epochs	900 epochs	90 epochs	270 epochs	900 epochs	
ResNet-50	Baseline	76.0	76.9 (+0.9)	75.9 (-0.1)	82.5	82.9 (+0.4)	81.6 (-0.9)
	+ Sigmoid	76.3 (+0.3)	77.8 (+1.8)	76.9 (+0.9)	83.0 (+0.5)	83.9 (+1.4)	82.7 (+0.2)
	+ Clean	76.4 (+0.4)	77.8 (+1.8)	77.4 (+1.4)	82.8 (+0.3)	83.7 (+1.2)	83.3 (+0.8)
	+ Both	76.6 (+0.6)	78.2 (+2.2)	78.5 (+2.5)	83.1 (+0.6)	84.3 (+1.8)	84.1 (+1.6)
ResNet-101	Baseline	77.4	77.6 (+0.2)	76.4 (-1.0)	83.7	83.6 (-0.1)	81.9 (-1.8)
	+ Sigmoid	77.8 (+0.4)	78.2 (+0.8)	77.3 (-0.1)	84.2 (+0.5)	84.2 (+0.5)	82.7 (-1.0)
	+ Clean	77.9 (+0.5)	79.2 (+1.8)	78.6 (+1.2)	84.0 (+0.3)	84.6 (+0.9)	84.0 (+0.3)
	+ Both	78.0 (+0.6)	79.5 (+2.1)	79.2 (+1.8)	84.3 (+0.6)	85.1 (+1.4)	84.4 (+0.7)
ResNet-152	Baseline	78.0	78.3 (+0.3)	77.1 (-0.9)	84.1	83.8 (-0.3)	82.3 (-1.8)
	+ Sigmoid	78.5 (+0.5)	78.7 (+0.7)	77.4 (-0.6)	84.6 (+0.5)	84.3 (+0.2)	82.7 (-1.4)
	+ Clean	78.6 (+0.6)	79.6 (+1.6)	79.0 (+1.0)	84.4 (+0.3)	85.0 (+0.9)	84.4 (+0.3)
	+ Both	78.7 (+0.7)	79.8 (+1.8)	79.3 (+1.3)	84.6 (+0.5)	85.2 (+1.1)	84.5 (+0.4)

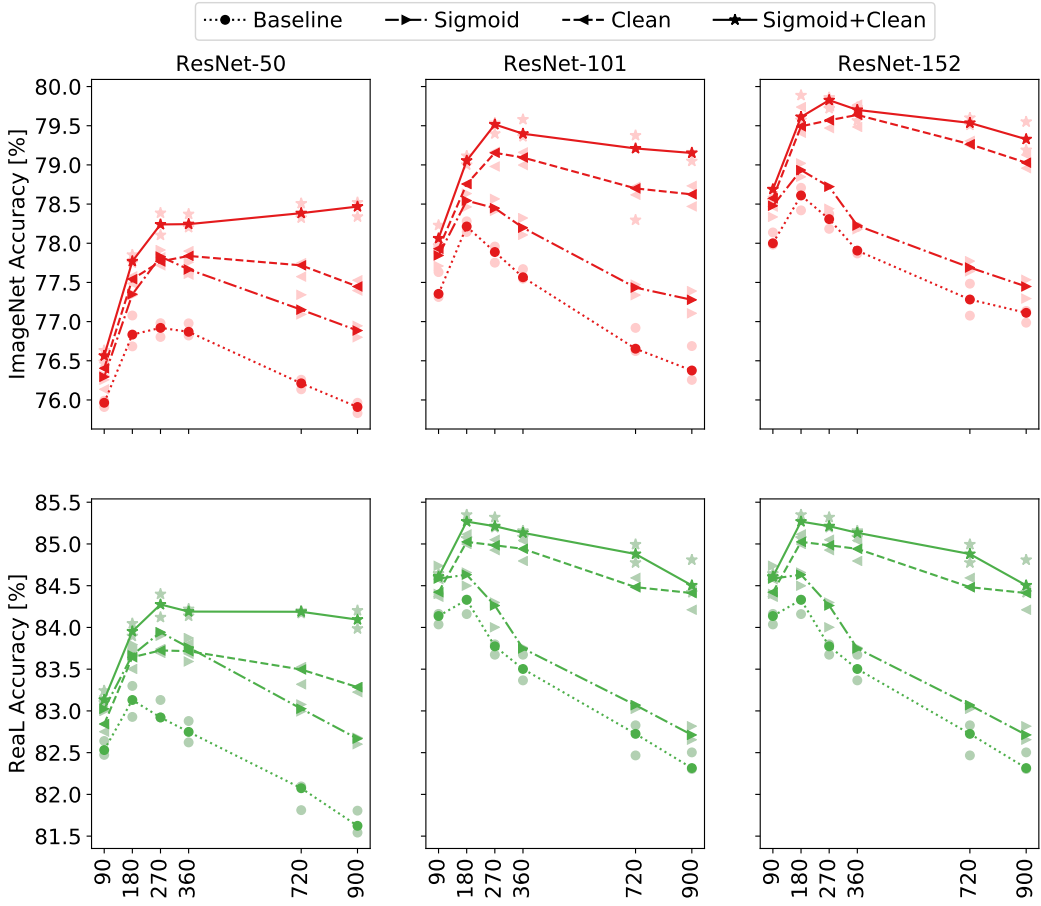


Figure 8: Top-1 accuracy (in percentage) on ImageNet with our proposed sigmoid loss and clean label set. X-axis shows the training epochs. The above row shows results on the original ImageNet labels, and the bottom row shows the RealL accuracy for the models. The curve shows the median results across three runs, where we use light color to mark the other two runs. Either sigmoid loss or clean label set leads to consistent improvements over the baseline (standard cross-entropy loss with softmax on the all original ImageNet images) and using both results in the best accuracies.

C ReaL accuracies of all models in Fig. 4

Table 5: ReaL and “original” ILSVRC-2012 top-1 accuracies (in percent) of all models used for Fig. 4 in the main paper, sorted by their ReaL accuracies.

Ref.	Model	ReaL Acc.	Orig. Acc.
self	Top-3 Ensemble [39, 30, 41]	91.20	89.03
[39]	NoisyStudent-L2	90.55	88.38
[30]	BiT-L	90.54	87.55
[1]	ILSVRC-2012 labels	90.02	100.0
[41]	Fix-ResNeXt-101, 32x48d, IG	89.73	86.36
[29]	ResNeXt-101, 32x48d, IG	89.11	85.40
[30]	BiT-M	89.02	85.40
[31]	Assemble ResNet-152	88.65	84.19
[35]	CPC v2, fine-tuned (100%)	88.33	83.25
[29]	ResNeXt-101, 32x8d, IG	88.19	82.65
[31]	Assemble ResNet-50	87.82	82.76
[32]	NASNet-A Large	87.56	82.60
[34]	S4L MOAM	86.59	80.32
[33]	Once for all (Large)	86.02	79.95
[28]	ResNeXt-101, 32x8d	85.18	79.18
[4]	ResNet-152	84.79	78.24
[27]	Inception v3	83.58	77.18
[34]	S4L-Rotation (100%)	83.10	76.72
[4]	ResNet-50	82.94	76.10
[37]	SimCLR	82.82	76.56
[34]	S4L-Exemplar (100%)	81.26	74.41
[32]	NASNet-A Mobile	81.15	73.92
n/a	VGG-16 + BatchNorm	80.60	73.34
[34]	S4L MOAM (10%)	80.41	73.22
[35]	CPC v2, fine-tuned (10%)	80.28	72.90
[3]	VGG-16	79.01	71.56
[35]	CPC v2, linear	78.67	71.49
[36]	MoCo v2, long	78.23	71.02
[34]	S4L-Exemplar (10%)	69.76	62.21
[34]	S4L-Rotation (10%)	69.05	61.37
[2]	AlexNet	62.88	56.36